Raman spectroscopy of natural oxalates

R. L. Frost•

Inorganic Materials Research Program, Queensland University of Technology, 2 George Street, Brisbane, GPO Box 2434, Queensland 4001, Australia.

Published as:
Frost, R.L., Raman spectroscopy of natural oxalates. Analytica Chimica Acta, 2004. 517(1-2): p. 207-214.

Abstract

Oxalates are markers or indicators of environmental events. Oxalates are readily determined by Raman spectroscopy. Thus deterioration of works of art, biogeochemical cycles, plant metal complexation, the presence of pigments and minerals formed in caves can be analysed. A comparative study of a suite of natural oxalates including weddellite, whewellite, moolooite, humboldtine, glushinskite, natroxalate and oxammite has been undertaken using Raman spectroscopy. The minerals are characterised by the wavenumber of the CO stretching vibration which is cation sensitive. The band is observed at 1468 cm^{-1} for weddellite, 1489 cm^{-1} for moolooite, 1471 cm^{-1} for glushinskite and 1456 cm^{-1} for natroxalate. Except for oxammite, the infrared and Raman spectra are mutually exclusive indicating that the minerals are bidentate. Differences are also observed in the wavenumber of the water OH stretching bands of the minerals. The significance of this work rests with the ability of Raman spectroscopy to identify oxalates which often occur as films on a host rocks or works of art.

Keywords: oxalate, weddellite, moolooite, humboldtine, natroxalate, oxammite, glushinskite, Raman spectroscopy, infrared spectroscopy

Introduction

The presence of oxalates is widespread in nature, not only in plants but also as naturally occurring minerals. Minerals may be formed in for example bat guano in caves. These minerals form as the result of expulsion of heavy metals from fungi, lichens and plants [1-3]. Recently Frost et al. found oxalic acid in the art works of Australian aboriginals. The caves near Chillagoe in Queensland hold very ancient aboriginal works of art. In the primitive paintings oxalic acid was found. It is probable that certain plants were used to make the mineral pigments such as hematite and kaolinite to stick to the cave walls [4]. The production of simple organic acids such as oxalic and citric acids has profound implications for metal speciation in biogeochemical cycles [5]. The metal complexing properties of the acids are essential to the nutrition of fungi and lichens and affect the metal stability and mobility in the environment [5]. Lichens and fungi produce the oxalates of heavy metals as a mechanism for the removal of heavy metals from the plant [6]. Recently, Macnish

• Author to whom correspondence should be addressed (r.frost@qut.edu.au)

and others identified intracellular calcium oxalate crystals in Geraldton wax flowers (*Chamelaucium uncinatum*) Schauer (Myrtaceae). These authors considered that the complexation of the oxalic acid with calcium controlled the concentration of heavy metals in the plant. Importantly the crystals were < 1 μm in size and were very difficult to identify other than by Raman spectroscopy. The presence of these oxalate crystals appears to have an effect similar to that found in cacti [7]. Among the oxalates are the two calcium oxalates known as weddellite (the dihydrate) and whewellite (monohydrate). Ca-oxalate exists in two well-described modifications: as the more stable monoclinic monohydrate whewellite and the less stable tetragonal dihydrate weddellite. Weddelite serves for lichens as a water absorbing and accumulating substrate which transforms to whewellite when humidity drops. Such minerals are important in human physiology as the minerals are found in the urinary tract [8, 9]. Many other divalent oxalates exist in nature. The magnesium based oxalate is known as glushinskite [10, 11]. The copper oxalate is known as moolooite [2, 12] and the ferrous oxalate as humboldtine [13, 14]. These three oxalates are also the product of lichen growth. Two natural univalent oxalates are known. These are the oxalates of sodium and ammonium known as natroxalate and oxammite [15].

The presence of oxalates provides evidence for the deterioration of works of art [16-18] and carbon dating has been used to estimate the age of the works of art [19]. The presence of the oxalates has been used as an indicator of climate change [20]. The presence of pigments in ancient works of art effected the growth of lichens on the art works [21]. In calcareous artifacts such as the famous Chinese terra cotta soldiers or Egyptian epigraphs, the formation of Ca-oxalate layers leads to the destruction of the surface and to deterioration of the historian works of art. But in places where the surface is covered by some blue colours (Egyptian and Chinese Blue, Chinese Purple) the growth of lichens is inhibited and the artifacts are well preserved. The copper ion contained in the pigments is responsible for this effect since copper is a strong poison for micro-organisms [21]. Weddellite and whewellite very often occur together with gypsum on the surface of calcareous artifacts exposed in the Mediterranean urban environment, as main constituents of reddish patinas called in Italy 'scialbatura'. The origin of this is a matter of controversy. The observation of the interface between calcite substratum and the above mentioned secondary minerals is an important step in the explanation of alteration process of artifacts of historic and artistic interest [22]. Studies of the black paint have shown the presence of oxalates in the paint with serious implications for remediation [23]. The use of infrared and Raman spectroscopy for the study of oxalates originated with the necessity to study renal stones [24, 25]. FT Raman spectroscopy has been used to study urolithiasis disease for many years, and the ethiopathogenesis of stone formation is not well understood [26].

Whilst there have been several studies of synthetic metal oxalates [27-33], few studies of natural oxalates have been forthcoming and no comprehensive comparison of the natural oxalates has been undertaken. The study of natural oxalates as opposed to synthetic oxalates is of importance in the study of the environment as oxalates act as markers for significant environmental events. Few studies of the spectroscopy of water in these minerals have been forthcoming. The objective of this work is to undertake a comparative study using a combination of Raman and infrared spectroscopy of a suite of common natural oxalates.

EXPERIMENTAL

Minerals:

The minerals used in this study were obtained from Australian museums and are known as 'type' minerals.

Whewellite Registered Sample Number M5531 originated from Burg River, near Dresden, Saxony, Germany.

Humboldtine Sample Number M13748 originated from Bohemia, Czech Republic

Natroxalate Sample Number M46430 originated from Alluaiv Mtn., Lovozero Massif, Kola peninsula, Russia.

Weddellite originated from the Weddell Sea, Antarctica.
Moolooite originated from Murchison, Mooloo Downs Station**,** Western Australia
Oxammite originated from Guanape Island Peru.

The samples were phase analyzed using X-ray diffraction and the compositions checked using EDX measurements.

Raman microprobe spectroscopy

The crystals of the oxalate minerals were placed and orientated on the stage of an Olympus BHSM microscope, equipped with 10x and 50x objectives and part of a Renishaw 1000 Raman microscope system, which also includes a monochromator, a filter system and a Charge Coupled Device (CCD). Raman spectra were excited by a HeNe laser (633 nm) at a resolution of 2 cm^{-1} in the range between 100 and 4000 cm^{-1}. Repeated acquisition was used to improve the signal to noise ratio. Spectra were calibrated using the 520.5 cm^{-1} line of a silicon wafer. Further details of the experimental procedure have been published [34-40].

Spectroscopic manipulation such as baseline adjustment, smoothing and normalisation were performed using the Spectracalc software package GRAMS (Galactic Industries Corporation, NH, USA). Band component analysis was undertaken using the Jandel 'Peakfit' software package, which enabled the type of fitting function to be selected and allows specific parameters to be fixed or varied accordingly. Band fitting was done using a Gauss-Lorentz cross-product function with the minimum number of component bands used for the fitting process. The Gauss-Lorentz ratio was maintained at values greater than 0.7 and fitting was undertaken until reproducible results were obtained with squared correlations of R^2 greater than 0.995.

RESULTS AND DISCUSSION

Factor group analysis

Aqueous oxalate is uncoordinated and will be of point group D_{2d}. Thus the vibrational activity is given by $\Gamma = 3A_1 + B_1 + 2B_1 + 3E$. Thus all modes are Raman active and the $2B_1 + 3E$ modes are infrared active. All oxygens in the structure are

equivalent and hence only one symmetric stretching mode should occur. Upon coordination of the oxalate as a mono-oxalato species as will occur in the natural minerals, the symmetry species is reduced to C_{2v}. The irreducible expression is then given by $\Gamma = 6A_1 + 2A_2 + 5B_1 + 2B_2$. Hence all modes are both Raman and infrared active. In this situation both the symmetric and antisymmetric stretching modes will be observed. If two moles of oxalate are bonded to the cation in a planar arrangement then the molecular point group will be D_{2h} and the irreducible representation is given by $\Gamma = 7A_g + 3B_{1g} + 3B_{2g} + 5B_{3g} + 3A_u + 7B_{1u} + 7B_{2u} + 4B_{3u}$. The first four modes are Raman active (namely $7A_g + 3B_{1g} + 3B_{2g} + 5B_{3g}$) and the last four modes are infrared active (namely $3A_u + 7B_{1u} + 7B_{2u} + 4B_{3u}$). Under this symmetry, there is a centre of symmetry which means the infrared and Raman bands are exclusive.

Raman spectra of the CO stretching region

The Raman spectra of the 1200 to 1800 cm^{-1} region is shown in Figure 1. The results of the Raman spectroscopic analysis together with the band assignments are given in Table 1. A band is identified in all the spectra in the 1456 to 1473 cm^{-1} range and is assigned to the $\nu_{(C-O)}$ stretching mode. The wavenumber of this band was identified at 1449 cm^{-1} for potassium oxalate in the solid state [30]. For weddellite and humboldtine the band was observed at 1468 cm^{-1}. It is possible to discriminate between hydration states of calcium oxalate; the monohydrate (whewellite) featured a v(CO) stretching band at 1493 cm^{-1} whereas the dihydrate (weddellite) had a v(CO) stretching band at 1475 cm^{-1}. The band was observed for moolooite at 1489 cm^{-1}. Moolooite is the bis copper(II) oxalate and the natural sample contains no water of hydration. Previous studies of the dihydrate copper(II) oxalate observed the v(CO) at 1495 cm^{-1} [30]. The Raman spectrum of the mineral glushinskite shows a band at 1471 cm^{-1}. The spectrum for natroxalate shows a band at 1456 cm^{-1}, a wavenumber which is comparatively low compared with those of other natural oxalates. Natroxalate is similar to that of moolooite in that no water of crystallisation is found for the natural mineral.

The Raman spectra of many of the minerals show additional bands on the low wavenumber side of the symmetric stretching mode. Bands are observed at 1411 cm^{-1} for weddellite and whewellite, 1433 cm^{-1} for moolooite, 1450 cm^{-1} for humboldtine, 1454 cm^{-1} for glushinskite. For oxammite additional bands are observed at 1451, 1447 and 1430 cm^{-1}. It is suspected that these additional bands are also assignable to the symmetric stretching modes; but of molecular species other than the bis-oxalate complexes. Another possibility is that these bands are due to the B_{2g} mode, which is the OCO wag. The wavenumber of this band is identified at 1392 cm^{-1} for aqueous potassium oxalate and at 1348 cm^{-1} for potassium oxalate in the solid state. A band is observed in this work at 1358 cm^{-1} for natroxalate. Bands which may also be attributable to the OCO wag are observed at 1417 and 1312 cm^{-1} for oxammite.

Infrared spectrum of the CO stretching region

The infrared spectra of the suite of minerals are shown in Figure 2. The results of the infrared spectral analysis reported in Table 2. A comparison of figures 1 and 2 confirm the rule of mutual exclusion for the spectroscopy of these natural oxalates. No bands are observed in the infrared spectra round 1460 cm^{-1} and no intense bands are observed in the Raman spectra around 1600 cm^{-1}, although some

low intensity bands are observed in this region in Figure 1. The exception is oxammite where bands are observed in both the Raman and infrared spectra around 1400 cm^{-1}. For aqueous oxalate the antisymmetric stretching (B_{2u}) mode is observed at 1600 cm^{-1}. For weddellite and whewellite two bands are observed at 1623 and 1605 cm^{-1}. The IR spectrum of humboldtine shows a single band centred at 1615 cm^{-1}. For moolooite the band is observed at 1632 cm^{-1} and is strongly asymmetric and component bands may be resolved at 1722, 1679, 1632 and 1602 cm^{-1}. For glushinskite bands are observed at 1679, 1660, 1634 and 1603 cm^{-1}. The IR spectrum of natroxalate shows bands at 1675, 1628 and 1604 cm^{-1}. Published IR data suggest that there should be a single band at 1632 cm^{-1} [30]. The reason for multiple antisymmetric stretching modes for each of the minerals is unclear; suffice to express that multiple species may be present. For example many oxalate minerals polymerise [41, 42]. The mineral oxammite fits well into this category. Multiple bands are observed in the infrared spectrum for both the symmetric and antisymmetric stretching modes.

The infrared spectra show quite intense bands centred around 1300 cm^{-1}. These bands may be assigned to B_{3u} OCO stretching mode. For weddellite and whewellite bands are observed at 1366 and 1309 cm^{-1}. For moolooite two intense bands are observed at 1317 and 1361 cm^{-1} with low intensity bands at 1352, 1311 and 1279 cm^{-1}. A band was observed at 1365 cm^{-1} and assigned to the OCO stretching mode for synthetic copper(II) oxalate dihydrate [41, 42]. Both humboldtine and glushinskite show a similar infrared pattern to moolooite with component bands at 1312 and 1357; 1314 and 1369 cm^{-1} respectively. The IR spectrum of natroxalate shows strong intensity at 1337 and 1314 cm^{-1} with low intensity bands at 1416, 1400, 1296 and 1251 cm^{-1}. The infrared spectrum of oxammite shows bands at 1288 and 1308 cm^{-1}. The reason for the multiplicity of bands cannot be attributed to a reduction in symmetry and loss of degeneracy but rather to the presence of more than one structure. It is possible for oxammite that not only the di-oxalate but the poly-oxalate, mono-oxalate and free oxalate are present in varying degrees of concentration.

Raman spectrum of the C-C stretching region

The Raman spectrum of the 800 to 1100 cm^{-1} region is shown in Figure 3. A Raman band is observed at around 900 cm^{-1} and is assigned to the ν(C-C) stretching mode. The band is observed at 909 cm^{-1} for weddellite, 921 cm^{-1} for moolooite, 913 cm^{-1} for humboldtine, 915 cm^{-1} for glushinskite, 892 cm^{-1} for oxammite and for natroxalate at 884 cm^{-1}, which corresponds well with the published value of 888 cm^{-1} for solid potassium oxalate. It should be noted that there is a large shift (~40 cm^{-1}) for the C-C stretching vibration between the 'free' oxalate and the oxalate in these natural oxalates. A second intense band is observed for natroxalate is observed at 875 cm^{-1}. This implies a non-equivalence of the C-C stretching vibrations. The Raman spectra of the oxalate minerals all show a low intensity band at around 860 cm^{-1}. The band is observed at 868 cm^{-1} for weddellite, 833 cm^{-1} for moolooite, 856 cm^{-1} for humboldtine, 861 cm^{-1} for glushinskite, 866 cm^{-1} for oxammite. The band is assigned to the OCO bending mode. A band is not observed at this wavenumber for potassium oxalate.

The infrared spectrum of the 500 to 1000 cm^{-1} region is shown in Figure 4. The C-C stretching mode does not give rise to a band or is only a very low intensity

band in the infrared spectrum. Two low intensity bands are observed at 884 and 957 cm^{-1}. Whewellite shows only a single band at 917 cm^{-1}. The IR spectrum of moolooite shows a very weak band at 917 cm^{-1}. Humboldtine has a band at a similar wavenumber and oxammite a band at 871 cm^{-1}. An intense band is observed for weddellite at 779 cm^{-1} with a strong shoulder at 762 cm^{-1}. The infrared spectrum of whewellite shows a broad band centred upon 820 cm^{-1}. The IR spectrum of natroxalate shows two strong bands at 818 and 766 cm^{-1}. These bands are assigned to the OCO bending modes which are strong in the infrared spectrum and of low intensity in the Raman spectrum.

Raman spectrum of the deformation modes of oxalate

The Raman spectrum of the low wavenumber region is shown in Figure 5. Raman bands are observed for weddellite and whewellite at 596 and 505 cm^{-1}. Natroxalate has Raman bands at 567 and 481 cm^{-1}. The band at 596 cm^{-1} is broad and of low intensity, and is attributed to water librational modes. The band at 505 cm^{-1} for the calcium oxalates and at 481 cm^{-1} for the sodium oxalate may be attributed to the symmetric OCO bending mode. For humboldtine the bands are observed at 582 and 518 cm^{-1}. The Raman spectrum of moolooite shows more complexity with bands observed at 610, 584 and 558 cm^{-1}. Such complexity was observed in the Raman spectrum of a synthetic copper(II) oxalate dihydrate [43]. In this work, Raman bands were observed at 616, 591, 563 and 498 cm^{-1}. Raman bands were observed at 642, 489 and 438 cm^{-1} for oxammite.

Figure 5 also shows some quite intense bands in the 100 to 300 cm^{-1} range. Both weddellite and whewellite show bands at 259, 220, 188 and 162 cm^{-1}. One possible assignment is that the bands are due to CaO stretching and bending vibrations. The intensities of the bands for natroxalate are weak. For moolooite bands are observed at 290 and 209 cm^{-1}. These bands may be assigned to the CuO stretching and bending modes respectively. The position of the bands differs slightly from that published for the copper(II) oxalate dihydrate [43]. Intense bands are observed for glushinskite and humboldtine at 310, 265, 237 and 226 cm^{-1}, and 293, 246 and 203 cm^{-1} respectively. The Raman spectrum of oxammite is quite complex with multiple bands observed at 278, 224, 210, 198, 181 and 160 cm^{-1}.

Raman spectra of the OH stretching region.

It is interesting that many papers report the spectroscopy of oxalates but fail to mention the spectroscopy of the water of crystallisation in the oxalate minerals. The Raman spectrum of the hydroxyl stretching region for the natural oxalates is shown in Figure 6. Firstly moolooite and natroxalate do not have any water of crystallisation, and have no Raman bands in the OH stretching region. The Raman spectra of weddellite and whewellite are different in the OH stretching region. Two bands are observed for weddellite at 3467 and 3266 cm^{-1} whereas bands are observed for whewellite at 3462, 3359, 3248 and 3067 cm^{-1}. The Raman spectrum of the hydroxyl stretching region of glushinskite shows a sharp intense band at 3367 cm^{-1} with low intensity bands at 3391 and 3254 cm^{-1}. The Raman spectrum of oxammite in this region shows complexity with the overlap of the OH and NH stretching vibrations. Two bands are observed at 3235 and 3030 cm^{-1} and are

assigned to the OH vibrations. Bands observed at 2995, 2900 and 2879 cm^{-1} are attributed to the NH vibrational modes.

The patterns of the OH stretching vibrations observed in the Raman spectra are reflected in the infrared spectra (Figure 7). The spectra of weddellite and whewellite are different. The infrared spectrum of weddellite shows OH stretching vibrations at 3593, 3450, 3337, 3248 and 3089 cm^{-1}. The infrared spectrum of whewellite shows a broad pattern. No spectrum is observed for natroxalate and a low intensity broad band observed for moolooite in all probability relates to adsorbed water. The infrared spectrum of glushinskite and humboldtine show intense bands at 3389 and 3472 cm^{-1} respectively. Low intensity bands are observed for glushinskite at 3380, 3360, 3305, 3230 and 3126 cm^{-1}. Low intensity bands are observed for humboldtine at 3312 and 3136 cm^{-1}. In the case of oxammite infrared bands are observed at 3195, 3186 and 3053 cm^{-1} and are attributed to the water OH stretching vibrations. The infrared bands observed at 2978, 2856, 2840, 2630 and 2344 cm^{-1} are assigned to NH stretching vibrations. It is probable that the large number of bands observed in the NH stretching region is ascribed to the non-planar nature of oxammite [44]. It has been suggested that the oxalate is twisted around the C-C bond by some 28 ° [45].

Conclusions

A suite of natural oxalate minerals has been characterised by both Raman and infrared spectroscopy. Each oxalate mineral has its own characteristic spectrum with the minerals weddellite and whewellite showing strong similarities in their spectra except for the water OH stretching region and in the very low wavenumber region. The minerals are characterised by the wavenumber of the CO stretching vibration which is cation sensitive. The band is observed at 1468 cm^{-1} for weddellite, 1489 cm^{-1} for moolooite, 1471 cm^{-1} for glushinskite and 1456 cm^{-1} for natroxalate. Both natroxalate and moolooite are characterised by the lack of water OH stretching vibrations. The wavenumber of the symmetric and antisymmetric stretching vibrations is characteristic of the particular oxalate and it is suggested that the position of the bands depends on the size and polarity of the cation.

The significance of this work rests with the ability of Raman spectroscopy to identify oxalates which often occur as films on a host rocks or works of art. The oxalates act as markers or indicators of environmental events. The deterioration of works of art may be determined through the presence of oxalates. The presence of the oxalates may also provide a mechanism for remediation. If life existed on Mars at some time in the past or even exists in the present time, low life forms such as fungi and lichens may exist. Such organisms may be found in very hostile environments [46-48]. Lichens and fungi can control their heavy metal intake through expulsion as metal salts such as oxalates. The presence of these oxalates may be used as a marker for the pre-existence of life. The interpretation of the spectra of natural oxalates is important in these types of study.

Acknowledgments

The financial and infra-structure support of the Queensland University of Technology Inorganic Materials Research Program is gratefully acknowledged. The

Australian Research Council (ARC) is thanked for funding. Prof Allan Pring of the South Australian Museum, Mr Ross Pogson of The Australian Museum and Mr Dermot Henry of Museum Victoria are thanked for the loan of the oxalate minerals.

References

[1]. H. J. Arnott and M. A. Webb, Scanning Electron Microsc. (1983) 1747.
[2]. J. E. Chisholm, G. C. Jones and O. W. Purvis, Mineralogical Magazine 51 (1987) 715.
[3]. A. Frey-Wyssling, Am. J. Bot. 68 (1981) 130.
[4]. R. L. Frost, Z. Ding and H. D. Ruan, Journal of Thermal Analysis and Calorimetry 71 (2003) 783.
[5]. G. M. Gadd, Mineralogical Society Series 9 (2000) 57.
[6]. T. Wadsten and R. Moberg, Lichenologist 17 (1985) 239.
[7]. P. V. Monje and E. J. Baran, Plant Physiology 128 (2002) 707.
[8]. J. P. Pestaner, F. G. Mullick, F. B. Johnson and J. A. Centeno, Archives of Pathology & Laboratory Medicine 120 (1996) 537.
[9]. J. Dubernat and H. Pezerat, J. Appl. Crystallogr. 7 (1974) 387.
[10]. H. Pezerat, J. Dubernat and J. P. Lagier, C. R. Acad. Sci., Paris, Ser. C 288 (1968) 1357.
[11]. M. J. Wilson and P. Bayliss, Mineralogical Magazine 51 (1987) 327.
[12]. R. M. Clarke and I. R. Williams, Mineralogical Magazine 50 (1986) 295.
[13]. K. Rezek, J. Sevcu, S. Civis and J. Novotny, Casopis pro Mineralogii a Geologii 33 (1988) 419.
[14]. E. Manasse, Rend. accad. Lincei 19 (1911) 138.
[15]. H. Winchell and R. J. Benoit, Am. Mineralogist 36 (1951) 590.
[16]. A. Piterans, D. Indriksone, A. Spricis and A. Actins, Proceedings of the Latvian Academy of Sciences, Section B: Natural, Exact and Applied Sciences 51 (1997) 254.
[17]. M. Del Monte and C. Sabbioni, Environ. Sci. Technol. 17 (1983) 518.
[18]. M. Del Monte and C. Sabbioni, Science of the Total Environment 50 (1986) 165.
[19]. J. Girbal, J. L. Prada, R. Rocabayera and M. Argemi, Radiocarbon 43 (2001) 637.
[20]. S. Moore, M. J. Beazley, M. R. Mccallum and J. Russ, Preprints of Extended Abstracts presented at the ACS National Meeting, American Chemical Society, Division of Environmental Chemistry 40 (2000) 4.
[21]. I. Lamprecht, A. Reller, R. Riesen and H. G. Wiedemann, Journal of Thermal Analysis 49 (1997) 1601.
[22]. R. Alaimo and G. Montana, Neues Jahrbuch fuer Mineralogie, Abhandlungen 165 (1993) 143.
[23]. G. Alessandrini, L. Toniolo, F. Cariati, G. Daminelli, S. Polesello, A. Pozzi and A. M. Salvi, Studies in Conservation 41 (1996) 193.
[24]. H. Moenke, Chem. Erde 21 (1961) 239.
[25]. M. Daudon, M. F. Protat, R. J. Reveillaud and H. Jaeschke-Boyer, Kidney Int. 23 (1983) 842.
[26]. C. Paluszkiewicz, M. Galka, W. Kwiatek, A. Parczewski and S. Walas, Biospectroscopy 3 (1997) 403.
[27]. R. I. Bickley, H. G. M. Edwards and S. J. Rose, Journal of Molecular Structure 243 (1991) 341.

[28]. H. Chang and P. J. Huang, Analytical Chemistry 69 (1997) 1485.
[29]. D. Duval and R. A. Condrate, Sr., Applied Spectroscopy 42 (1988) 701.
[30]. H. G. M. Edwards, D. W. Farwell, R. Jenkins and M. R. D. Seaward, Journal of Raman Spectroscopy 23 (1992) 185.
[31]. I. I. Kondilenko, P. A. Korotkov, N. G. Golubeva, V. A. Klimenko and A. I. Pisanskii, Optika i Spektroskopiya 45 (1978) 819.
[32]. O. I. Kondratov, E. A. Nikonenko, I. I. Olikov and L. N. Margolin, Zhurnal Neorganicheskoi Khimii 30 (1985) 2579.
[33]. T. A. Shippey, Journal of Molecular Structure 63 (1980) 157.
[34]. R. L. Frost, Spectrochimica Acta, Part A: Molecular and Biomolecular Spectroscopy 59A (2003) 1195.
[35]. R. L. Frost, M. Crane, P. A. Williams and J. T. Kloprogge, Journal of Raman Spectroscopy 34 (2003) 214.
[36]. R. L. Frost, W. Martens, P. A. Williams and J. T. Kloprogge, Journal of Raman Spectroscopy 34 (2003) 751.
[37]. R. L. Frost, P. A. Williams, J. T. Kloprogge and W. Martens, Neues Jahrbuch fuer Mineralogie, Monatshefte (2003) 433.
[38]. W. Martens, R. L. Frost, J. T. Kloprogge and P. A. Williams, Journal of Raman Spectroscopy 34 (2003) 145.
[39]. W. Martens, R. L. Frost and P. A. Williams, Journal of Raman Spectroscopy 34 (2003) 104.
[40]. R. L. Frost, W. Martens, P. A. Williams and J. T. Kloprogge, Mineralogical Magazine 66 (2002) 1063.
[41]. H. G. M. Edwards and P. H. Hardman, Journal of Molecular Structure 273 (1992) 73.
[42]. H. G. M. Edwards and I. R. Lewis, Spectrochimica Acta, Part A: Molecular and Biomolecular Spectroscopy 50A (1994) 1891.
[43]. H. G. M. Edwards, D. W. Farwell, S. J. Rose and D. N. Smith, Journal of Molecular Structure 249 (1991) 233.
[44]. N. A. Chumaevskii and O. U. Sharopov, Zhurnal Neorganicheskoi Khimii 33 (1988) 1914.
[45]. R. J. H. Clark and S. Firth, Spectrochimica Acta, Part A: Molecular and Biomolecular Spectroscopy 58A (2002) 1731.
[46]. H. G. M. Edwards, E. M. Newton and J. Russ, Journal of Molecular Structure 550-551 (2000) 245.
[47]. H. G. M. Edwards, N. C. Russell, M. R. D. Seaward and D. Slarke, Spectrochimica Acta, Part A: Molecular and Biomolecular Spectroscopy 51A (1995) 2091.
[48]. H. G. M. Edwards, N. C. Russell and M. R. D. Seward, Spectrochimica Acta, Part A: Molecular and Biomolecular Spectroscopy 53A (1997) 99.
[49]. J. Fujita, A. E. Martell and K. Nakamoto, The Journal of Chemical Physics 36 (1962) 324.

Ca	Cu	Fe^{2+}	Mg	Na	NH_4		
weddellite	moolooite	humboldtine	glushinskite	natroxalate	oxammite	Infrared [49]	Band assignments
3467 3266		3315	3391 3367 3254		3235 3030		$\nu_{s/}\ \nu_a$ (OH)
					2995 2900 2879		$\nu_{s/}\ \nu_a$ NH
					2161 1902		
1737	1673	1708	1720	1750	1737		
1628	1614	1555	1660 1636 1612	1643 1614	1695 1605	1632	ν_a (C=O)
1475	1514						ν_a (C=O)
1468	1489	1468	1471	1456	1473 1451 1447 1430	1433	ν_s (C-O) + ν (C-C)
1411	1433	1450	1454	1358	1417 1312	1302	ν_s (C-O) + δ(O-C=O)
1055 1053	1120						
909	921	913	915		892	890	ν_s (C-O) + δ(O-C=O)
868	831	856	861	884 875	866 815		ν_s (C-O)/ δ(O-C-O)

			657		642	785	δ(O-C=O) + ν(M-O)
596	610 584	582	585	567		622	Water libration
505	558	518	527			519	ν(M-O) + ν (C-C)
			521		489	519	Ring deform + δ(O-C=O)
				481	438	428 419	ν(M-O) + ring deform
						377 364	δ(O-C=O) + ν (C-C)
259	290	293	310		278	291	Out of plane bends
220	209	246	265 237 226		224		Lattice modes
188		203	221	221 156 117	210 198 181 160		Lattice modes
162							

Table 1 Raman spectroscopic analysis of natural oxalates

Ca	Cu	Fe^{2+}	Mg	Na	NH_4		
weddellite	moolooite	humboldtine	glushinskite	natroxalate	oxammite	Infrared [49]	Band assignments
3593 3450 3337 3248 3089	3529 3347 2971	3472 3312 3136	3389 3380 3360 3305 3230 3126		3195 3186 3053		$\nu_{s/}\ \nu_a$ (OH)
					2978 2856 2840 2630 2344		$\nu_{s/}\ \nu_a$ NH
					1900		
1623 1605	1722 1679 1632 1602	1615	1679 1660 1634 1603	1675 1628 1604	1701 1651 1582 1527	1632	ν_a (C=O)
1500	1574 1543 1512	1514 1479	1580	1538			ν_a (C=O)
1399	1430				1466 1447 1425	1433	ν_s (C-O) + ν (C-C)
1366 1309	1361 1352 1317	1357 1312	1369 1322 1314	1416 1400 1337	1410 1308 1288	1302	ν_s (C-O) + δ(O-C=O)

	1311 1279	1301 1266	1169	1314 1296 1251			
917						890	ν_s (C-O) + δ(O-C=O)
779 762	820 798	818 766 715	827 803	780 771 756	800 716	785	δ(O-C=O) + ν(M-O)
601			684		635 617	622	Water libration
						519	ν(M-O) + ν (C-C)
						519	Ring deform + δ(O-C=O)

Table 2 IR spectroscopic analysis of natural oxalates

LIST OF FIGURES

LIST OF TABLES

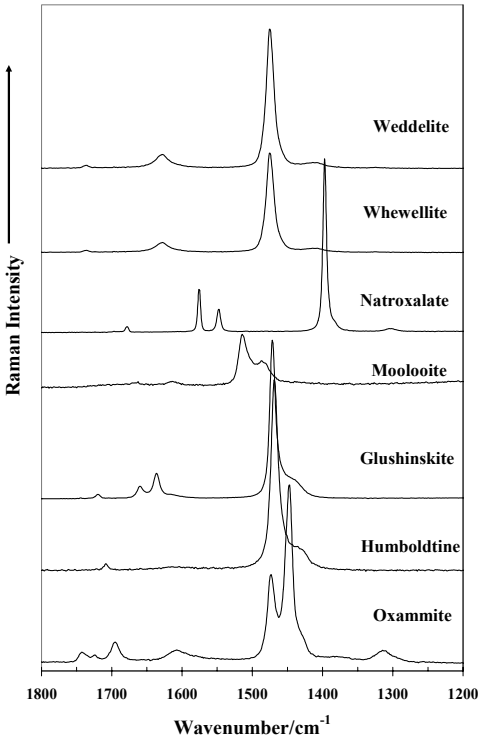

Figure 1 Frost

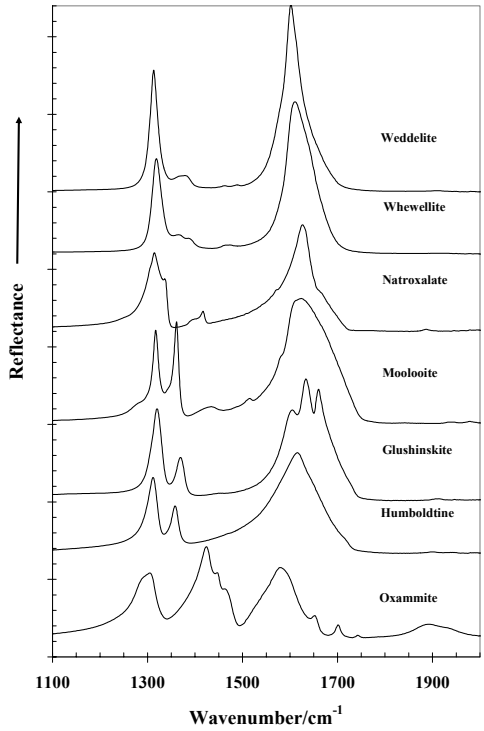

Figure 2 Frost

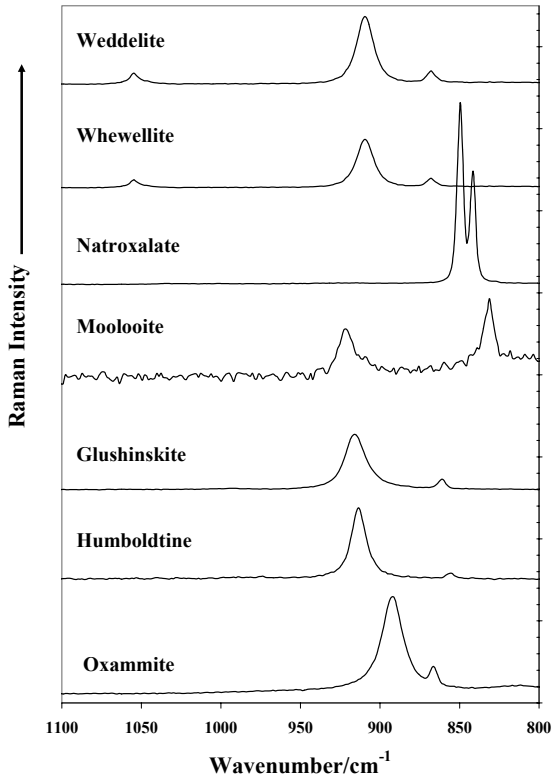

Figure 3 Frost

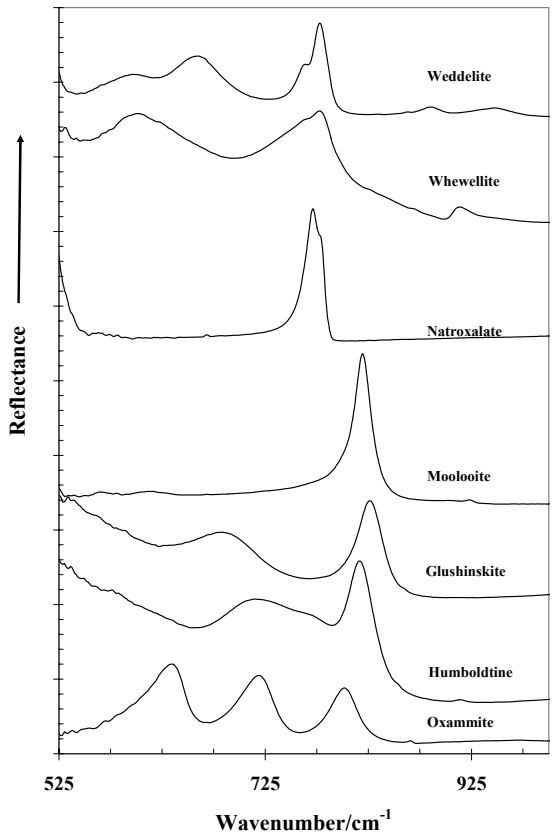

Figure 4 Frost

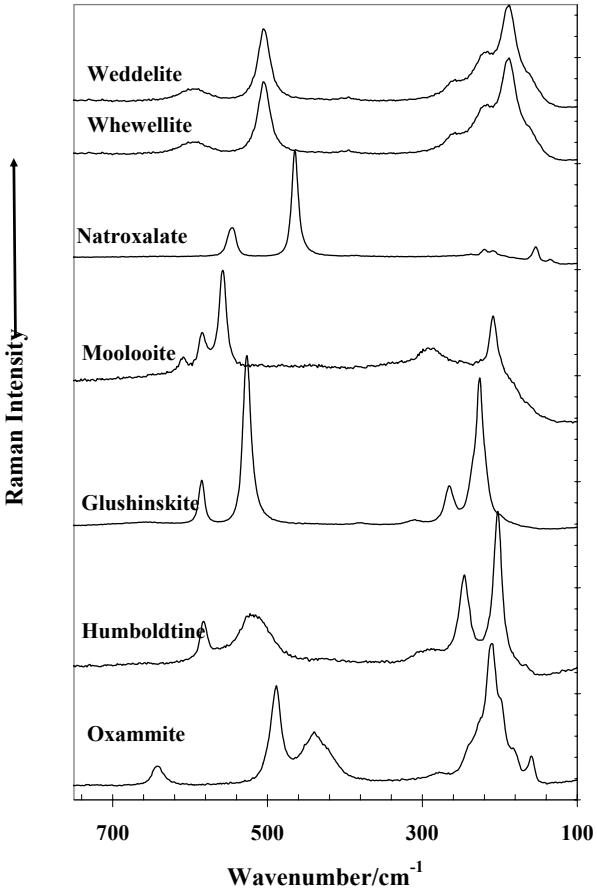

Figure 5 Frost

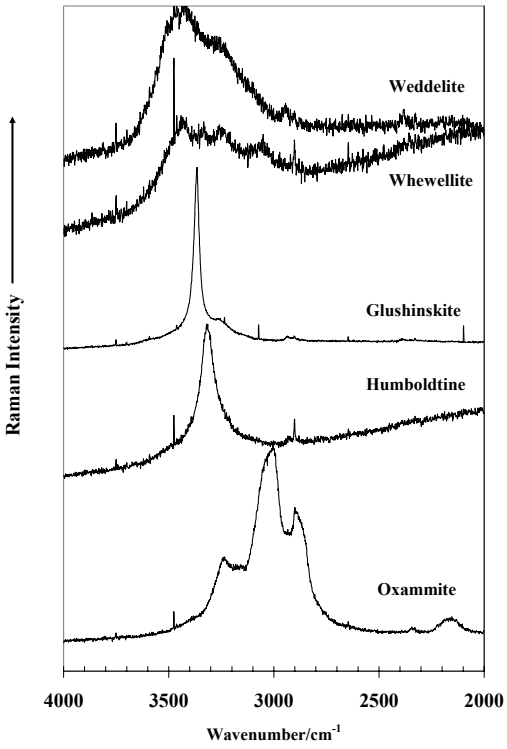

Figure 6 Frost

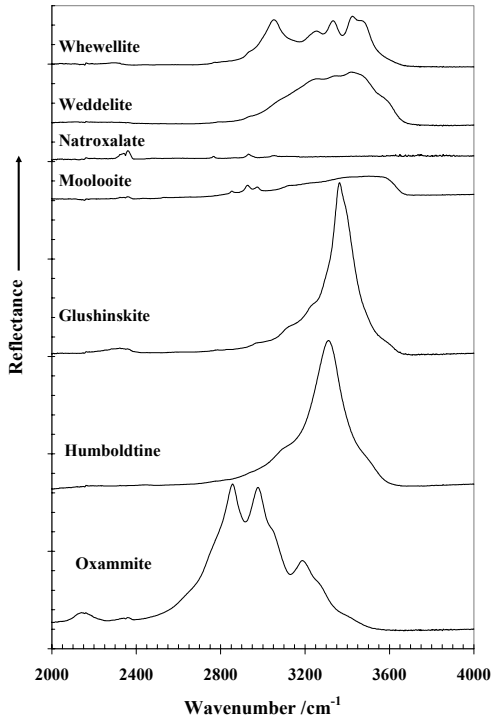

Figure 7 Frost